Progress In Electromagnetics Research B, Vol. 30, 313–335, 2011

MUTUAL CONVERSION OF TM_{mn} AND TE_{mn} WAVES BY PERIODIC AND APERIODIC WAVEGUIDE FILTERS COMPOSED OF DENSE METAL-STRIP GRATINGS

V. R. Tuz[1, 2, *], S. L. Prosvirnin[1, 2], and V. B. Kazanskiy[2]

[1]Institute of Radioastronomy of National Academy of Sciences of Ukraine, 4, Krasnoznamennaya st., Kharkiv 61002, Ukraine

[2]School of Radio Physics, Karazin Kharkiv National University, 4, Svobody Square, Kharkiv 61077, Ukraine

Abstract—The mutual conversion of the TM_{mn} and TE_{mn} waves ($m, n \neq 0$) in periodic and aperiodic (fractal-like) stratified waveguide structures composed of dense metal-strip gratings is studied. The stopbands and passbands conditions of Bloch waves, the reflection and transmission spectra of the periodic structure are examined versus the gratings parameters. Peculiarities of the wave localization, self-similarity and scalability of both reflected and transmitted spectra of the fractal-like structure are investigated. The appearance of additional peak multiplets in stopbands is revealed and a correlation of their properties with the parameter of grating filling is established.

1. INTRODUCTION

The unique features of periodical structures define their multipurpose using. The most known structures with simple periods are the sequences of dielectric layers which found wide applications as optical and microwave devices [1–5]. They are parts of distributed Bragg reflectors, antireflection coatings, interferometers, lasers, antennas, filters, absorber materials and many others. Further functionality expansion of the above-mentioned devices is provided by introducing inside of the structure's period the reactive, conductive and polarization-sensitive elements like rods, rings, discs, pins, strips, irises, etc. [6–16].

Received 18 April 2011, Accepted 13 May 2011, Scheduled 19 May 2011

* Corresponding author: Vladimir R. Tuz (tvr@rian.kharkov.ua).

The sequences of single- or double-spacing equally oriented metal-strip gratings (one- and two-element diaphragms) are widely used in waveguides to realize the bandpass filtration [17–20]. However in fact of the strong dispersion of the scattering coefficients of these diaphragms, the obtained filters usually have too narrow stopbands and low maximal attenuation between adjacent passbands. The dense metal-strip gratings ($æ = l/\lambda \ll 1$, where l is the grate period and λ is the wavelength) are deprived of these disadvantages. Therefore the diaphragms with the great number of elements are more appropriate for the frequency filtration [21–24]. The introduction of the polarization-sensitive multiple-element diaphragms (anisotropic semi-transparent screens [25–28]) inside of a waveguide additionally allows obtaining the modal filtration which is especially important in multimode transmission lines.

In the present paper a model of a multi-section frequency-modal filter is considered. The structure consists of magnetodielectric layers and polarization-sensitive semi-transparent screens. In contrast to the sequences of the dense screens considered earlier [21–24], we provide our studies in both single-mode and double-mode regimes of the wave propagation in a rectangular waveguide. The structure under study realizes the frequency-modal selection and the mutual conversion of the TM_{mn} and TE_{mn} waves ($m, n \neq 0$) in a waveguide. We will consider both perfectly periodic and aperiodic systems. The last one is the fractal-like (Cantor-like) multilayer [29–34]. It is known that the periodicity disturbance of a layered isotropic one-dimensional sample produces appearing additional high-Q resonances (localized modes) in the stopbands. These resonances in the case of structure with polarization-sensitive screens can be used for realization of the narrow-bandpass polarization filtration. On the other hand, the fractal-like structure can be considered as a structure with plural disturbances, and, furthermore, they exhibit certain distinctive features like the scalability and the self-similarity of the reflection and transmission spectra.

Modeling of the filter is achieved through the generalized transfer-matrices analysis. To determine the transfer-matrix of the structure's period the boundary-value problem is solved using the Weinstein-Sivov boundary conditions [25–28] which approximate the dense metal-strip grating with a thin anisotropic screen. The goal of the paper is to study the peculiarity of the polarization transformation of the TM_{mn} and TE_{mn} waves in a layered waveguide filter and especially to demonstrate the distinctive features of the waves localization in an aperiodic structure configuration.

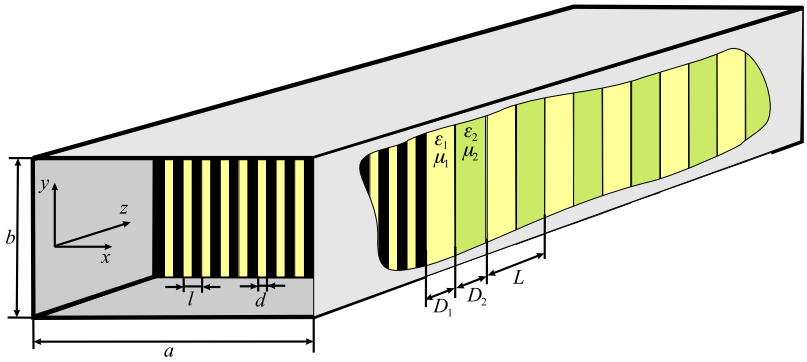

Figure 1. Periodic sequence of magnetodielectric layers and dense metal-strip gratings in a rectangular waveguide.

2. FIELDS. BOUNDARY CONDITIONS

First we consider a perfectly periodic in the z-axis direction, with period L, structure which consists of N identical metal-dielectric elements placed in a rectangular ($a \times b$) waveguide (Figure 1). Each of periods consists of two ($j = 1, 2$) homogeneous magnetodielectric layers with thicknesses D_j and material parameters ε_j, μ_j, and a dense ($æ = l/\lambda \ll 1$) metal-strip grating placed on the boundaries $z = \nu L$ ($\nu = 0, 1, \ldots, N-1$). The fillings of the input ($z \leq 0$) and output ($z \geq NL$) waveguide sections are homogeneous, isotropic and have permittivities ε_0, μ_0.

In general, the field scattered by the grating consists of the superposition of the infinite number of the partial waveguide waves. When the grate period l is much less than the wavelength λ, the field scattered by the grating is possible to describe using the Lamb approximation [35]. Under this approximation, only one of TE_{0n} or TE_{m0} waves (single-mode regime) or two TE_{mn} and TM_{mn} waves with the same indexes m, n (the double-mode regime) propagate in the waveguide structure. In the latter case, one of this wave is belonging to the type of the excitation field when the other appears as a result of the polarization transformation.

In the general case, as the excitation fields, the TM_{mn} and TE_{mn} waves in a waveguide are selected. The time dependence is defined in the form $\exp(-i\omega t)$ and omitted. The fields inside of the input, output and periodic waveguide sections are defined via the longitudinal components of the electric ($s = e$) and magnetic ($s = h$) Hertz vectors

$\vec{\Pi}_j^s = \vec{z}_0 \Pi_j^s$:

$$\begin{cases} \Pi_0^s = C_0^s \{A_0^s e^{i\gamma_0 z} + B_0^s e^{-i\gamma_0 z}\}\Phi^s, & z \le 0, \\ \Pi_{\nu j}^s = C_j^s \{A_{\nu j}^s e^{i\gamma_j [z-(\nu-1)L]} + B_{\nu j}^s e^{-i\gamma_j [z-(\nu-1)L]}\}\Phi^s, & 0 \le z \le NL, \\ \Pi_3^s = C_0^s A_3^s e^{i\gamma_0 (z-NL)}\Phi^s, & z \ge NL, \end{cases} \quad (1)$$

where C_j^s $(j = 0, 1, 2)$ are some constants which are defined from the normality conditions (see Appendix A), $\Phi^e = \Phi_{\alpha\alpha} = \sin(k_x x)\sin(k_y y)$ and $\Phi^h = \Phi_{\beta\beta} = \cos(k_x x)\cos(k_y y)$ are rectangular waveguide eigenwave functions of TM and TE waves, respectively, $\gamma_j = \sqrt{k_j^2 - g_{mn}^2}$ are wave propagation constants, $k_j = k\sqrt{\varepsilon_j \mu_j}$ are the wavenumbers, and $g_{mn}^2 = k_x^2 + k_y^2 = (\pi m/a)^2 + (\pi n/b)^2$ is the modal cut-off wavenumber for the TM_{mn} and TE_{mn} modes. The field components obtained from (1) are presented in Appendix A.

We use the Weinstein-Sivov boundary conditions [25–27] for the description of sufficiently thin gratings [28]:

$$\begin{aligned} E_{xj} &= E_{x(j+1)}, \\ E_{yj} &= E_{y(j+1)}, \\ iE_{yj}U^+ &= H_{x(j+1)} - H_{xj} + i\frac{M}{k}\frac{\partial}{\partial y}\left(\varepsilon_j E_{zj} - \varepsilon_{j+1} E_{z(j+1)}\right), \quad (2) \\ H_{yj} - H_{y(j+1)} &= iU^- \left[E_{x(j+1)} + i\frac{M}{k}\frac{\partial}{\partial y}\left(\mu_{j+1} H_{z(j+1)}\right)\right], \end{aligned}$$

where $U^+ = -(\mu_j + \mu_{j+1})/[\mu_j \mu_{j+1} æ \ln(0.5(1+u))]$, $U^- = æ(\varepsilon_j + \varepsilon_{j+1})\ln(0.5(1-u))$, $M = (\mu_j + \mu_{j+1})/[\mu_j \mu_{j+1}(\varepsilon_j + \varepsilon_{j+1})]$, and $u = \cos(\pi d/l)$ is the parameter of grating filling. The parameter u changes in the range $[-1, 1]$, where $u = -1$ corresponds to the absence of the grating and $u = 1$ corresponds to the metallic screen.

These boundary conditions are obtained using the rigorous problem solution of the plane monochromatic wave diffraction on the infinite periodic metal-strip grating placed on the interface between two magnetodielectric half-spaces. They describe the grating as an infinitely thin uniaxial anisotropic screen which anisotropy axis is directed along the y-axis. This model of the semi-transparent anisotropic screen excludes the modes interconversion within the wave type. However in the regime under study (the double-mode regime) the grating changes the initial proportion between the power of the TE_{mn} and TM_{mn} waves with the same indexes m, n (degenerate waves) in the transmitted and reflected fields.

3. METHOD OF SOLUTION. TRANSFER MATRIX

The structure under study is considered as a consecutive junction of the eight-poles which are equivalent to the structure periodic cells. They are described with the transfer matrix $\mathbf{T}$. In turn, each of the periodic cells consists of two elements which correspond to the first ($\mathbf{T}_1$) and second ($\mathbf{T}_2$) layers, ($\mathbf{T} = \mathbf{T}_1\mathbf{T}_2$). Note that the first element ($\mathbf{T}_1$) of the each periodic cell consists of the boundary with the grating (Figure 1). The matrix equation coupling the field amplitudes at the input and output of the corresponding eight-pole is obtained as follow:

$$\mathbf{V}_\nu = \{\mathbf{T}_1\mathbf{T}_2\}\mathbf{V}_{\nu+1} = \mathbf{T}\mathbf{V}_{\nu+1}, \tag{3}$$

where $\mathbf{V}_\nu = \{A^h_\nu\ B^h_\nu\ A^e_\nu\ B^e_\nu\}^T$ and $\mathbf{V}_{\nu+1} = \{A^h_{\nu+1}\ B^h_{\nu+1}\ A^e_{\nu+1}\ B^e_{\nu+1}\}^T$ are the vectors containing the field amplitudes at the eight-pole input and output; the upper index T is the matrix transpose operator. In the 2×2 block representation, the transfer-matrices of the first ($\mathbf{T}_1$), second ($\mathbf{T}_2$) and periodic ($\mathbf{T}$) elements, respectively, are:

$$\mathbf{T}_1 = \begin{pmatrix} \mathbf{T}_1^{hh} & \mathbf{T}_1^{he} \\ \mathbf{T}_1^{eh} & \mathbf{T}_1^{ee} \end{pmatrix}, \mathbf{T}_2 = \begin{pmatrix} \mathbf{T}_2^{hh} & 0 \\ 0 & \mathbf{T}_2^{ee} \end{pmatrix}, \mathbf{T} = \begin{pmatrix} \mathbf{T}^{hh} & \mathbf{T}^{he} \\ \mathbf{T}^{eh} & \mathbf{T}^{ee} \end{pmatrix}. \tag{4}$$

The elements of the transfer-matrices $\mathbf{T}_1$ and $\mathbf{T}_2$ are determined by solving the boundary-value problem related to the field components (A3) and are given in Appendix B.

Rising the matrix $\mathbf{T}$ to the power N gives the relation on the fields at the input and output of the whole structure:

$$\mathbf{V}_0 = \mathbf{T}_\Sigma\mathbf{V}_{N+1}, \tag{5}$$

where $\mathbf{T}_\Sigma = \mathbf{T}^N$, $\mathbf{V}_0 = \{A^h_0\ B^h_0\ A^e_0\ B^e_0\}^T$ and $\mathbf{V}_{N+1} = \{A^h_{N+1}\ 0\ A^e_{N+1}\ 0\}^T$ are the vectors containing the field amplitudes at the structure input and output.

The algorithm from the matrix polynomial theory [36] for raising the matrix $\mathbf{T}$ to the power N was introduced in [37] to study the structure with a large number of periods ($N \gg 1$)

$$\mathbf{T}_\Sigma = \sum_{p=1}^{4} \lambda_p^N \mathbf{F}_p. \tag{6}$$

Here λ_p are the eigenvalues of the transfer-matrix $\mathbf{T}$, $\mathbf{F}_p = \mathbf{P}\mathbf{I}_p\mathbf{P}^{-1}$, $\mathbf{P}$ is the matrix which columns are the set of independent eigenvectors of $\mathbf{T}$, $\mathbf{I}_p$ is the matrix with 1 in the (p, p) location and zeros elsewhere. The final result based on the formulas (5) and (6) is written as follow

$$\mathbf{V}_0 = \left\{ \sum_{p=1}^{4} \lambda_p^N \mathbf{F}_p \right\} \mathbf{V}_{N+1}. \tag{7}$$

In the structure under study two operating conditions can be provided. These conditions are different to the waveguide excitation with the TE_{mn} and TM_{mn} $(m, n \neq 0)$ or TE_{m0} and TE_{0n} waves. In the first case two types of waves in the waveguide structure propagate and their mutual conversion occurs. In the second case the wave conversion is absent and the elements of the non-diagonal blocks of the transfer matrix $\mathbf{T}$ are equal to zero. The equivalent scheme of the structure disintegrates into two autonomous transmission lines of a consecutive junction of the four-poles which are related to TE_{m0} and TE_{0n} waves. The transfer matrices of these four-poles coincide with one of two block-matrices $\mathbf{T}^{hh}$ or $\mathbf{T}^{ee}$ according to the wave type.

The behaviors and functional capabilities of the structure manifest itself in the reflection and transmission coefficients. For their determination, and taking into consideration the specificity of the double-mode regime, the equations coupling the field amplitudes at the structure input and output for the incident fields of the h-type $(A_0^e = 0)$ and the e-type $(A_0^h = 0)$ are written in the form:

$$\begin{aligned} \left\{A_0^h\ B_0^h\ 0\ B_0^e\right\}^T &= \mathbf{T}_\Sigma \left\{A_{N+1}^h\ 0\ A_{N+1}^e\ 0\right\}^T, \\ \left\{0\ B_0^h\ A_0^e\ B_0^e\right\}^T &= \mathbf{T}_\Sigma \left\{A_{N+1}^h\ 0\ A_{N+1}^e\ 0\right\}^T. \end{aligned} \tag{8}$$

Thus, the reflection and transmission coefficients of the reflected $(z \leq 0)$ and transmitted $(z \geq NL)$ fields are determined by the expressions $R^{ss} = B_0^s/A_0^s$, $\tau^{ss} = A_{N+1}^s/A_0^s$, and $R^{ss'} = B_0^{s'}/A_0^s$, $\tau^{ss'} = A_{N+1}^{s'}/A_0^s$ for the co-polarized and cross-polarized waves, respectively. From (8) they are:

$$\begin{aligned} R^{ee} &= \left(t_{11}t_{43} - t_{41}t_{13}\right)/\Delta, \quad \tau^{ee} = t_{11}/\Delta, \\ R^{eh} &= \left(t_{11}t_{23} - t_{21}t_{13}\right)/\Delta, \quad \tau^{eh} = -t_{13}/\Delta, \\ R^{hh} &= \left(t_{21}t_{33} - t_{23}t_{31}\right)/\Delta, \quad \tau^{hh} = t_{33}/\Delta, \\ R^{he} &= \left(t_{41}t_{33} - t_{43}t_{31}\right)/\Delta, \quad \tau^{he} = -t_{31}/\Delta, \end{aligned} \tag{9}$$

where $\Delta = t_{11}t_{33} - t_{31}t_{13}$, and t_{pq} are the elements of the transfer matrix $\mathbf{T}_\Sigma$.

4. BLOCH WAVES. REFLECTION AND TRANSMISSION SPECTRA OF PERIODIC STRUCTURE

The degree of the wave reflection and transmission in a selected frequency band depends on the eigenwave propagation conditions of the corresponding infinite periodic diaphragmatic waveguide structure.

In contrast to the single-mode regime, the solution of the diffraction problem of the TM_{mn} and TE_{mn} waves can not be derived in an analytical form like it is obtained in [22] for TE_{m0} and TE_{0n} waves. Thus, the numerical-analytical investigation of the parametric dependences of eigenvalues λ_p will be carried out.

The eigenvalues of the transfer-matrix, λ_p $(p = 1, 2, 3, 4)$, are the roots of the characteristic equation of the transfer matrix $\mathbf{T}$:

$$\det(\mathbf{T} - \lambda\mathbf{I}) = 0. \tag{10}$$

Since the matrix $\mathbf{T}$ is unimodular, Equation (10) comes to the following polynomial form:

$$\lambda^4 + S_3\lambda^3 + S_2\lambda^2 + S_1\lambda + S_0 = 0, \tag{11}$$

where $S_0 = \det \mathbf{T} = 1$, $S_1 = -\sum_{i=1}^{2}\sum_{j=i+1}^{3}\sum_{k=j+1}^{4}(m_{ii}m_{jj}m_{kk} + m_{ij}m_{jk}m_{ki} + m_{ik}m_{ji}m_{kj} - m_{ii}m_{jk}m_{kj} - m_{jj}m_{ki}m_{ik} - m_{kk}m_{ij}m_{ji})$, $S_2 = \sum_{i=1}^{3}\sum_{j=i+1}^{4}(m_{ii}m_{jj} - m_{ij}m_{ji})$, $S_3 = -\sum_{i=1}^{4} m_{ii}$ and $m_{\alpha\beta}$ are the elements of the matrix $\mathbf{T}$. If the coefficients of Equation (11) are satisfied by the equality $S_3 = S_1$, the left part of the dispersion equation of this type can be presented as the product of two quadratic polynomials [38–40]:

$$\left[\lambda^2 + Q_1\lambda + 1\right]\left[\lambda^2 + Q_2\lambda + 1\right] = 0 \tag{12}$$

The fact that the condition $S_3 = S_1$ is satisfied can be verified numerically. The coefficients of Equations (11) and (12) are related as

$$Q_1 + Q_2 = S_1, \quad 2 + Q_1Q_2 = S_2. \tag{13}$$

Expressing Q_1 and Q_2 through S_1 and S_2, we obtain

$$Q_{1,2} = \frac{S_1}{2} \pm \sqrt{\left(\frac{S_1}{2}\right)^2 + 2 - S_2}. \tag{14}$$

From (14) the eigenvalues of the transfer-matrix $\mathbf{T}$ are written in the form

$$\lambda_{1,2} = \frac{-Q_1 \pm \sqrt{Q_1^2 - 4}}{2} = -\frac{S_1}{4} - \sqrt{\left(\frac{S_1}{4}\right)^2 + \frac{2 - S_2}{4}} \pm \sqrt{\frac{1}{4}\left[\frac{S_1}{2} + \sqrt{\left(\frac{S_1}{2}\right)^2 + 2 - S_2}\right]^2 - 1}, \tag{15}$$

$$\lambda_{3,4} = \frac{-Q_2 \pm \sqrt{Q_2^2 - 4}}{2} = -\frac{S_1}{4} + \sqrt{\left(\frac{S_1}{4}\right)^2 + \frac{2 - S_2}{4}} \pm \sqrt{\frac{1}{4}\left[\frac{S_1}{2} + \sqrt{\left(\frac{S_1}{2}\right)^2 + 2 - S_2}\right]^2 - 1}, \quad (16)$$

Thus, the dispersion Equation (12) is split into two independent parts. From physical point of view it means that, in the waveguide structure, there are two independent spectra of eigenwaves, each of them is characterized by its dispersion relation and wavenumber.

For the infinite periodic structure the fields in the regular parts of the neighboring basic elements differ by the Floquet factor. Taking into account the transfer matrix definition (3), the following identity holds:

$$\mathbf{V}_\nu = \mathbf{T}\mathbf{V}_{\nu+1} = \exp(-i\Gamma L)\mathbf{V}_{\nu+1}, \quad (17)$$

where the constant Γ is the Bloch wavenumber. From (17) it follows that the eigenvalues of the basic element transfer matrix are related to the propagation constants of the Bloch waves via the condition $\lambda_j = \exp(\pm i\Gamma_j L)$; the sign choice for the jth type of wave corresponds to the wave propagation direction.

The obtained solution allows us to identify the passband (stopband) positions through analysis of the dependences of λ_p versus the frequency or structure parameters.

The values of $Q_{1,2}$ ($\lambda_{1,2}$, $\lambda_{3,4}$) defined by Expressions (14)–(16) determine the band spectrum of two pairs of eigenwaves. One pair of eigenwaves propagates in the positive direction of the z axis and the other has the opposite direction of propagation. The passbands are determined by the condition $|Q_1| \leq 2$ ($|\lambda_{1,2}| \leq 1$) for one eigenwave and $|Q_2| \leq 2$ ($|\lambda_{3,4}| \leq 1$) for another in each of these pairs. These conditions are displayed in Figure 2(a) as a shaded area. Since the dispersion Equation (12) consists of two independent factors, the bandwidth of these spectra can be mutually overlapped. There is a significant difference between these two solutions of the dispersion equation. It is because they correspond to two waves with different orientation of the vector $\vec{E}$ relatively to the metallic strips of gratings.

By this means, the eigenwaves of an unbounded periodical waveguide structure are the orthogonally polarized h and e waves, where the latter one is the wave which electric field vector $\vec{E}$ is oriented along the gratings elements. As a result, the gratings are capacitive and inductive diaphragms for the h and e waves, respectively. The first kind of diaphragms is transmissive, when the second one is highly reflective.

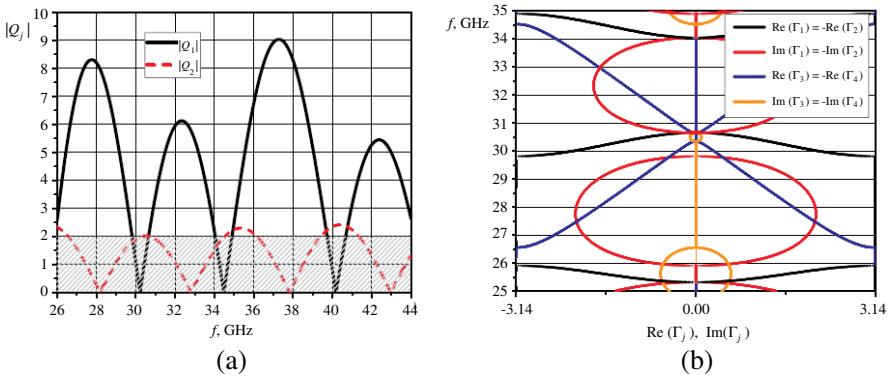

Figure 2. (a) Eigenwaves propagation conditions and (b) band spectrum of a periodic sequence of magnetodielectric layers and dense metal-strip gratings in a rectangular waveguide. The guide used for this work is the R120 (WR75) rectangular waveguide, $a = 19.0\,\text{mm}$, $b = 9.5\,\text{mm}$. Other parameters are: $m = n = 1$, $L = 20\,\text{mm}$, $D_1 = 10\,\text{mm}$, $u = -0.7$, $\varepsilon_0 = \varepsilon_2 = \mu_0 = \mu_1 = \mu_2 = 1$, $\varepsilon_1 = 4$.

This yields to different behaviors of the propagation conditions of eigenwaves. Thus, the e wave has very narrow passbands, and $|Q_1| > 2$ holds practically in all frequency range, whereas the passbands of the h wave are wide, and areas where $|Q_2| \leq 2$ prevails.

On the basis of obtained Equations (15) and (16), the propagation constants Γ_j $(j = 1, 2, 3, 4)$ of these two eigenwaves are calculated (Figure 2(b)). These propagation constants obey the conditions $\Gamma_1 = -\Gamma_2$ and $\Gamma_3 = -\Gamma_4$, where the sign defines the propagation direction along or opposite to the z axis. Thus, it is defined that Γ_1, Γ_2 and Γ_3, Γ_4 correspond to the e and h waves, respectively. One can see that the stopbands of the e and h waves are when $\text{Im}(\Gamma_1) = -\text{Im}(\Gamma_2) \neq 0$ and $\text{Im}(\Gamma_3) = -\text{Im}(\Gamma_4) \neq 0$.

The considered features of the eigenwaves propagation of the infinite periodic diaphragmatic waveguide determine the character of the frequency dependences of the reflection and transmission coefficients of the finite structure, which consists of N periods. First we consider the situation when the primary field is the TE_{10} or TE_{01} waves (Figure 3(a)). When $u < 0$, the passbands of the TE_{01} wave occupy practically whole frequency range. The bands positions of this wave are correspond to the propagation conditions of the h polarized eigenwave. Due to the finiteness of the structure and as the result of the waves interference, the boundaries of stopbands have a smooth shape and there are the spectrum oscillations in the passbands. The main distinctive features of the spectra of the TE_{10} wave are the facts

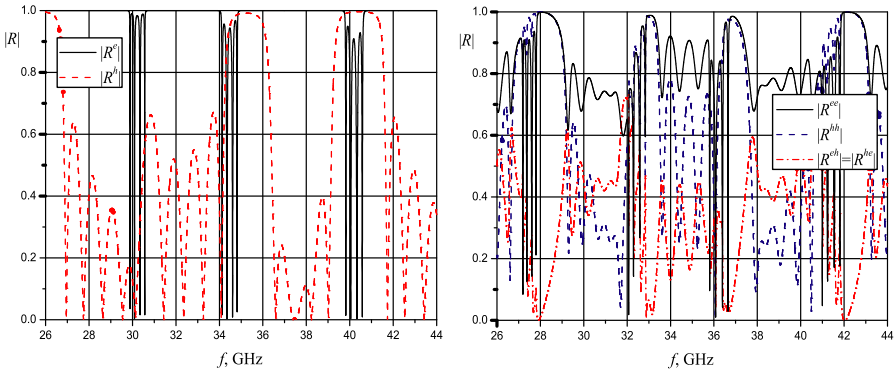

Figure 3. Frequency dependences of the reflection spectra of (a) TE_{01}, TE_{10} and (b) TE_{11}, TM_{11} waves; $a = 19.0\,\text{mm}$, $b = 9.5\,\text{mm}$, $L = 20\,\text{mm}$, $D_1 = 10\,\text{mm}$, $u = -0.7$, $N = 5$, $\varepsilon_0 = \varepsilon_2 = \mu_0 = \mu_1 = \mu_2 = 1$, $\varepsilon_1 = 4$.

that the stopbands are wide and they starting and finishing abruptly. The passbands are very narrow, and the oscillations here are sizable. Accordingly, for this type of wave, the bands positions are related to the propagation conditions of the e polarized eigenwave. Note, that stopbands of the TE_{01} wave correspond to passbands of the TE_{10} wave and vice versa. When u rises ($u > 0$), the gaps between the grating strips reduce and the structure becomes reflecting for both TE_{01} and TE_{10} waves.

The spectra of TE_{mn} and TM_{mn} waves incorporate the features of both h and e polarized eigenwaves. One can see that the spectra of TE_{11} and TM_{11} waves have characteristic bands of high reflection and transmission (Figure 3(b)). These bands primarily determined by the propagation conditions of the h polarized wave, and the high-Q resonances exist exactly within the passbands of the e wave. The degree of the polarization transformation in the reflected and transmitted fields depends on the topology of the primary field, namely, from the orientation of the transverse components of the field ($\vec{E}_\perp = \vec{x}_0 E_x + \vec{y}_0 E_y$, $\vec{H}_\perp = \vec{x}_0 H_x + \vec{y}_0 H_y$) related to the position of the gratings conducting strips which are directed along the y axis. Thus, if $|E_y| > |E_x|$ (as example, in the case of TM_{11} wave), the wave with the topology of the primary field prevails in the reflected field, i.e., $|R^{ee}| > |R^{eh}|$. When $|E_y| < |E_x|$ (in the case of TE_{11} wave) there is $|R^{hh}| < |R^{he}|$. Due to the symmetry of the transfer matrix coefficients, the magnitudes of the cross-polarized waves are equal to each other in the reflected and transmitted fields, $|R^{eh}| = |R^{he}|$, $|\tau^{eh}| = |\tau^{he}|$.

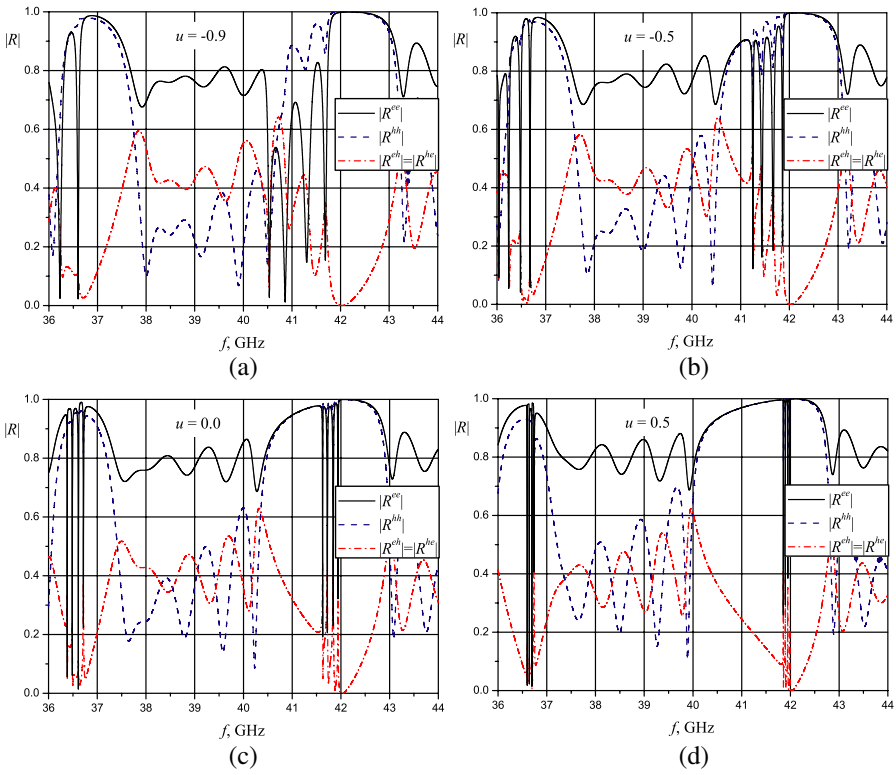

Figure 4. Frequency dependences of the reflection spectra of TE_{11}, TM_{11} waves versus the parameter of the gratings filling u; $a = 19.0\,\text{mm}$, $b = 9.5\,\text{mm}$, $L = 20\,\text{mm}$, $D_1 = 10\,\text{mm}$, $N = 5$, $\varepsilon_0 = \varepsilon_2 = \mu_0 = \mu_1 = \mu_2 = 1$, $\varepsilon_1 = 4$.

The reflection spectra dependences versus the parameter of the gratings filling u are given in Figure 4. As the parameter u increases, the reflectivity of the gratings rises which leads to the formation of broader stopbands and to increase the quality factor of resonances within these stopbands. Also, the curves of the reflection coefficient magnitudes for different configurations of the primary field m, n, are plotted in Figure 5. One can see that changing the field topology yields to the variation of the proportion between the co-polarized and cross-polarized components in the reflected field.

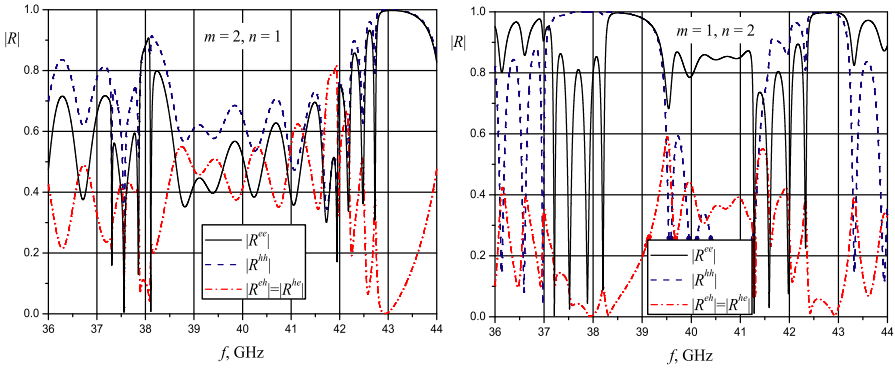

Figure 5. Frequency dependences of the reflection spectra of TE_{mn}, TM_{mn} waves for different configurations of the primary field; $a = 19.0\,\mathrm{mm}$, $b = 9.5\,\mathrm{mm}$, $L = 20\,\mathrm{mm}$, $D_1 = 10\,\mathrm{mm}$, $u = -0.7$, $N = 5$, $\varepsilon_0 = \varepsilon_2 = \mu_0 = \mu_1 = \mu_2 = 1$, $\varepsilon_1 = 4$.

5. REFLECTION AND TRANSMISSION SPECTRA OF FRACTAL-LIKE STRUCTURE

A particular emphasis in the theory of periodic structures is placed on the samples with periodicity defects. The defect inside a multilayer periodic structure produces additional localized resonances (localized modes) within stopbands. These localized modes are employed in the construction of filters with very narrow bandwidths. Generally a configuration of such resonances is dependent on the material parameters of the defective element and its position within the structure. It is apparent that the introduction of plural defects inside a periodic structure can significantly change the localized resonances features. As example of such structures with plural defects, the deterministic aperiodic (quasi-periodic) multilayers can be mentioned [29–33]. The main advantage of such deterministic aperiodic structures is the fact that the position of localized resonances can be obtained definitely [31]. One of such aperiodic structures is the fractal-like multilayer structure which is constructed according to the rule of generating of the Cantor set [29–31, 33].

The Cantor set is one of the simplest fractals, and it is a subset of the unit interval of the real line. The Cantor set is created by repeatedly deleting the open middle thirds of a set of line segments. One starts by deleting the open middle third (1/3, 2/3) from the interval [0, 1], leaving two line segments: [0, 1/3] ∪ [2/3, 1]. Next, the open middle third of each of these remaining segments is deleted,

leaving four line segments: $[0, 1/9] \cup [2/9, 1/3] \cup [2/3, 7/9] \cup [8/9, 1]$. This process can be continued ad infinitum. The fractal dimensionality of such triadic Cantor set is $\ln 2/\ln 3$. This Cantor set can be extended if it started from a larger interval, i.e., the fragmentation is provided on the another specified interval $[0, \Lambda]$.

A multilayer structure which is constructed in the form of such extended Cantor set, is characterized by two fundamental parameters, the generator $G = 3, 5, 7, \ldots$ and the generation number $N = 1, 2, 3, \ldots$. Sample structures are shown in Figure 6 and the stack construction can be understood from there. At the first stage, starting with an interval $[0, \Lambda]$ ($\Lambda = GL$ is the total thickness of the structure), certain parts are removed, forming a Cantor set of order $N = 1$ composed of the subsets $[0, L], \ldots, [(G-1)L, \Lambda]$ (yellow gaps) that are separated by intervals $[L, 2L], \ldots, [(G-2)L, (G-1)L]$ (green gaps). The Cantor set of order $N = 2$ is obtained by removing again certain parts of these subsets $\{[0, L/G], [2L/G, 3L/G], \ldots, [(G-1)L/G, L]\}$, $\{[2L, (2G+1)L/G], [(2G+2)L/G, (2G+3)L/G], \ldots, [(3G-1)L/G, 3L]\}, \ldots, \{[(G-1)L, ((G-1)+1)L/G], [((G-1)+2)L/G, ((G-1)+3)L/G], \ldots, [(G-1)(G+1)L/G, \Lambda]\}$. High-order sets are formed in similar ways. Note, that degree of this fragmentation is restricted by the Lamb approximation [35], i.e., the distance between the gratings must be enough to provide the attenuation of all partial waveguide waves except two orthogonally-polarized waves which coincide with the type of the excitation field.

It can be observed that the obtained subsets are copies of the

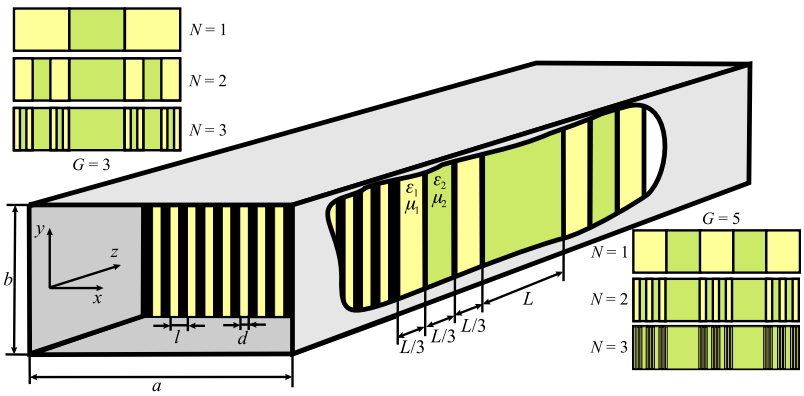

Figure 6. Self-similar Cantor set sequence of magnetodielectric layers and dense metal-strip gratings in a rectangular waveguide.

original set scaled by a factor of $1/G$. This property is called self-similarity. Two other properties are the recursive property and the formation of fine structures [33]. The recursive property comes from the fact that certain parts of each subset are removed when the order increases from N to $N+1$. The fine structure comes from the specific rule of subset formation with the result that it is possible to know the form of each subset at any order N. The fractal dimensionality of a Cantor set of any order N attributed to the structure under study is $\ln[(G+1)/2]/\ln G$ [30].

In view of the fact of the self-similarity of the fractal structure, the calculation algorithm for the determination of the total transfer matrix $\mathbf{T}_\Sigma = \mathcal{T}_N$ is constructed iteratively by the next formulae [33]:

$$\begin{cases} \mathcal{T}_0 = \mathbf{T}_2(\Lambda), \qquad N = 0, \\ \mathcal{T}_1 = [\mathbf{T}_1(L/G^{(N-1)})\mathbf{T}_2(L/G^{(N-1)})]^{(G-1)/2}\mathbf{T}_1(L/G^{(N-1)}), \\ \qquad\qquad\qquad\qquad\qquad\qquad N = 1, \\ \mathcal{T}_n = [\mathcal{T}_{n-1}\mathbf{T}_2(L/G^{(N-n)})]^{(G-1)/2}\mathcal{T}_{n-1}, \qquad n = 2 \ldots N. \end{cases} \tag{18}$$

Here the transfer matrices $\mathbf{T}_1$ and $\mathbf{T}_2$ are defined in (B1), in which the propagation matrices $\mathbf{P}_j$ $(j = 1, 2)$ are the functions of the variable length D.

The frequency dependences of the reflection and transmission spectra of a Cantor-like structure are periodic function (with the period divisible by G) with alternating bands of high and low average level of

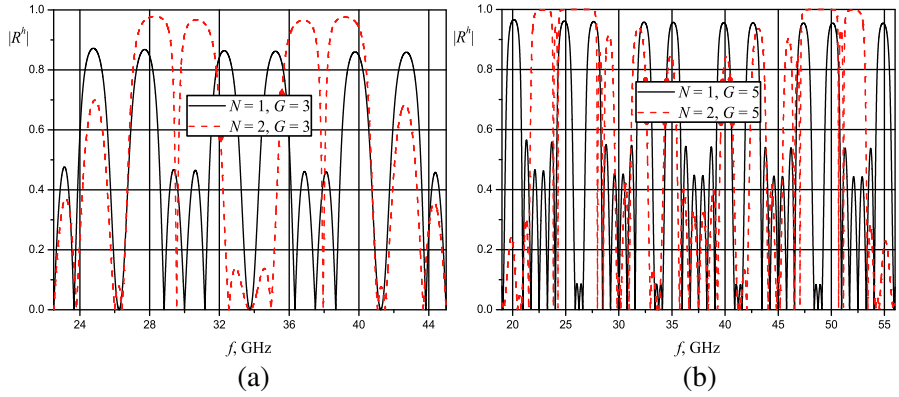

Figure 7. Frequency dependences of the reflection spectra of a Cantor-like structure of magnetodielectric layers and dense metal-strip gratings in a rectangular waveguide for different stages of fractal growth (G, N) in the case of TE_{01} wave; $a = 19.0\,\text{mm}$, $b = 9.5\,\text{mm}$, $L = 20\,\text{mm}$, $u = -0.7$, $\varepsilon_0 = \varepsilon_2 = \mu_0 = \mu_1 = \mu_2 = 1$, $\varepsilon_1 = 4$.

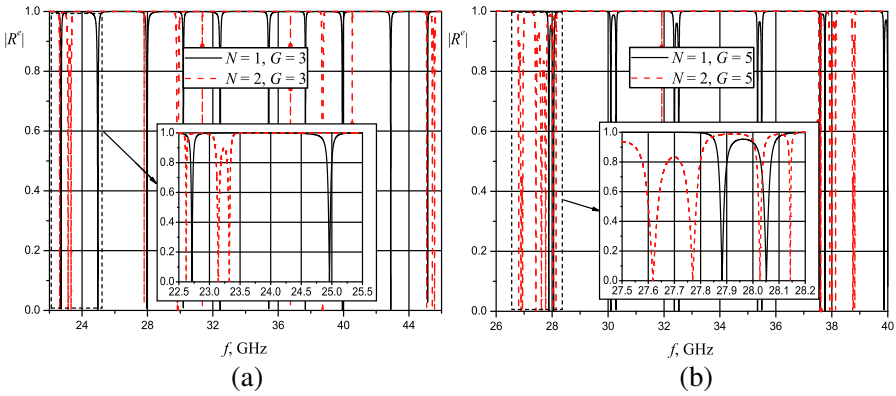

Figure 8. Frequency dependences of the reflection spectra of a Cantor-like structure of magnetodielectric layers and dense metal-strip gratings in a rectangular waveguide for different stages of fractal growth (G, N) in the case of TE_{10} wave; $a = 19.0\,\text{mm}$, $b = 9.5\,\text{mm}$, $L = 20\,\text{mm}$, $u = -0.95$, $\varepsilon_0 = \varepsilon_2 = \mu_0 = \mu_1 = \mu_2 = 1$, $\varepsilon_1 = 4$.

the reflection. In the theory of quasiperiodic and aperiodic structures it is conventional to term these bands as the quasi-stopbands and quasi-passbands (or pseudo-stopbands and pseudo-passbands). The spectra have self-similar properties, i.e., reflection coefficient variation at each higher stage is a modulated version of that associated with the previous stage [29].

If the primary field is the TE_{10} or TE_{01} waves (Figures 7, 8) the main characteristic features of the reflected spectra are similar to those ones of the periodic structure (Figure 3(a)). Thus, whereas the quasi-passbands of the TE_{01} are wide, they are very narrow for the TE_{10} wave even for weakly filled gratings ($u = -0.95$). Analogously, the stopbands of the TE_{01} wave correspond to passbands of the TE_{10} wave and vice versa. Nevertheless, the distinctive feature of the fractal-like structure is the formation of the sharp transmission resonances (peaks) inside the quasi-stopbands. It is well known that such kind of localized resonances (modes) appears in the periodic structures with defect. But the peculiar feature of these resonances relative to the fractal-like structure is their sequential splitting [30]. The last one appears as the interrelation between the generator G and the number of peaks (single or multiplets) in the quasi-stopbands. Thus the number of peaks in the multiplets equals $(G-1)/2$ and the total number of peaks in one period equals the number of layers, i.e., G^N. On can see in Figure 8 that, for the chosen structure generations, the number

of peaks doubles when the N rises, and the doublet and multiplet of peaks appear as the numbers G and N increase (see insets in Figure 8).

The reason of such splitting is understood from the point of view of self-similarity of Cantor-like structures regarded in terms of the coupled cavities [30, 33]. As an example, the sample stack ($G = 5$, $N = 2$) consists of three multilayer inclusions of ($G = 5$, $N = 1$) stacks. Each single peak in the spectrum of a ($G = 5$, $N = 2$) stack is a resonant mode produced by the layer with parameters ε_2, μ_2 (green 'cavity') with thickness L, splits into two modes because there are two such layers ('cavities') in a ($G = 5$, $N = 2$) stack.

The characteristic of the sequential splitting changes when a structure is excited with the TE_{mn} or TM_{mn} type of wave (Figure 9). Additional peaks appear in quasi-stopbands of both co-polarized and cross-polarized reflected fields. The position of these additional peaks corresponds to the frequency of the localized resonances of the orthogonally polarized e and h waves (see the appearance of additional peaks at the frequencies nearly 28 and 37 GHz in Figure 9(b)). This effect is explained by the composition of the eigenmodes of the multilayer structure sections separated with the homogeneous gaps, and by additional eigenmodes that appear as a result of the wave polarization transformation [33]. The quality-factor of the peaks and distance between them depend on the parameter of the grating filling u. Thus there is possibility to change the localized modes configuration via the appropriate choosing structure composition and grating filling.

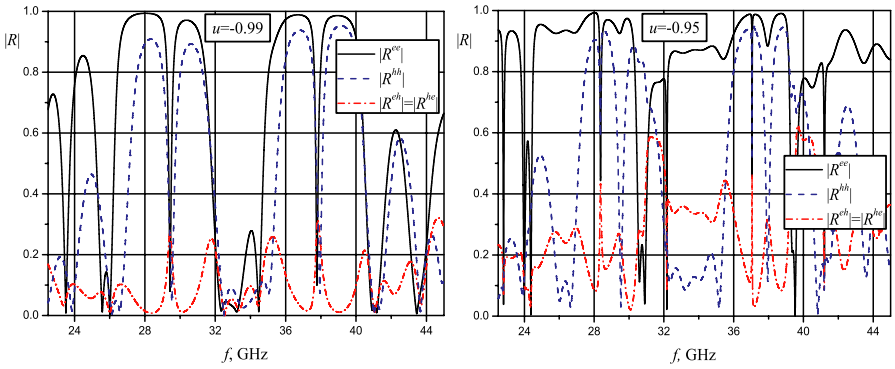

Figure 9. Frequency dependences of the reflection spectra of a Cantor-like structure of magnetodielectric layers and dense metal-strip gratings in a rectangular waveguide as function of the parameter of grating filling u in the case of TE_{11} and TM_{11} waves; $a = 19.0$ mm, $b = 9.5$ mm, $L = 20$ mm, $G = 3$, $N = 2$, $\varepsilon_0 = \varepsilon_2 = \mu_0 = \mu_1 = \mu_2 = 1$, $\varepsilon_1 = 4$.

6. CONCLUSION

In the present paper the reflection and transmission properties of the periodic and aperiodic multilayer waveguide structures are studied. The investigation is provided in the both single-mode and double-mode regimes when the structure is excited with TE_{10}, TE_{01} and TE_{mn}, TM_{mn} waves, respectively. The stopband and passband positions of the periodical structure are defined using the solution related to the Bloch waves. The reflection and transmission spectra of the periodic structure are examined versus the gratings parameters. The effect of the dense gratings on the mutual conversion of the TM_{mn} and TE_{mn} waves is shown.

As an aperiodic structure, the fractal-like (Cantor-like) stratified waveguide filter composed of metal-strip gratings is considered. Peculiarities of the wave localization, self-similarity, scalability and sequential splitting of both reflected and transmitted fields of the fractal-like structure are investigated. The appearance of additional peak multiplets in quasi-stopbands is revealed and a correlation of their properties with the gratings parameters is established.

The knowledge about spectral features of such systems is important to design the frequency-modal filters, polarization-sensitive loads, switching devices based on the nonlinear dielectrics in the case when the gratings strips are used as electrodes to which voltage is applied.

APPENDIX A.

In the general case, from (1), the longitudinal components of the electric $\vec{\Pi}^e = \{0, 0, \Pi^e(x, y)\}$ and the magnetic $\vec{\Pi}^h = \{0, 0, \Pi^h(x, y)\}$ Hertz vectors are defined as follows [12]:

$$\begin{aligned} \Pi^e &= C^e(A^e e^{i\gamma z} + B^e e^{-i\gamma z}) \sin k_x x \sin k_y y, \\ \Pi^h &= C^h(A^h e^{i\gamma z} + B^h e^{-i\gamma z}) \cos k_x x \cos k_y y, \end{aligned} \tag{A1}$$

The field components are governed by the coupled differential equations related to the Hertz vectors:

$$\begin{aligned} \vec{E} &= \operatorname{grad} \operatorname{div}\vec{\Pi}^e + k^2 \varepsilon\mu \vec{\Pi}^e + ik\mu \operatorname{rot}\vec{\Pi}^h, \\ \vec{H} &= -ik\varepsilon \operatorname{rot} \vec{\Pi}^e + \operatorname{grad} \operatorname{div}\vec{\Pi}^h + k^2 \varepsilon\mu \vec{\Pi}^h, \end{aligned} \tag{A2}$$

From (A1) and (A2) the components of vectors $\vec{E}$ and $\vec{H}$ are obtained as:

$$\begin{aligned}
E_x &= i\left[\gamma k_x C^e \left(A^e e^+ - B^e e^-\right) - k\mu k_y C^h \left(A^h e^+ + B^h e^-\right)\right] \Phi_{\beta\alpha},\\
E_y &= i\left[\gamma k_y C^e \left(A^e e^+ - B^e e^-\right) + k\mu k_x C^h \left(A^h e^+ + B^h e^-\right)\right] \Phi_{\alpha\beta},\\
E_z &= g^2 C^e \left(A^e e^+ + B^e e^-\right) \Phi_{\alpha\alpha},\\
H_x &= -i\left[k\varepsilon k_y C^e \left(A^e e^+ + B^e e^-\right) + \gamma k_x C^h \left(A^h e^+ - B^h e^-\right)\right] \Phi_{\alpha\beta},\\
H_y &= i\left[k\varepsilon k_x C^e \left(A^e e^+ + B^e e^-\right) - \gamma k_y C^h \left(A^h e^+ - B^h e^-\right)\right] \Phi_{\beta\alpha},\\
H_z &= g^2 C^h \left(A^h e^+ + B^h e^-\right) \Phi_{\beta\beta},
\end{aligned} \tag{A3}$$

where $\Phi_{\alpha\alpha} = \sin k_x x \sin k_y y$, $\Phi_{\beta\beta} = \cos k_x x \cos k_y y$, $\Phi_{\beta\alpha} = \cos k_x x \sin k_y y$, $\Phi_{\alpha\beta} = \sin k_x x \cos k_y y$, $e^{\pm} = \exp(\pm i\gamma z)$, and the constants C^s $(s = e, h)$ are defined from the next normality condition

$$\int_0^a \int_0^b \left[\vec{E} \times \vec{H}^*\right] d\vec{s} = \int_0^a \int_0^b \left(E_x H_y^* - E_y H_x^*\right) dxdy = 1, \tag{A4}$$

The substitution of field components (A3) into integral (A4) separately for e and h waves yields

$$\begin{aligned}
&(C^e)^2 \gamma k\varepsilon \int_0^a \int_0^b \left[k_x^2 \cos^2 k_x x \sin^2 k_y y + k_y^2 \sin^2 k_x x \cos^2 k_y y\right] dxdy\\
&= \frac{1}{4}(C^e)^2 abg^2 \gamma k\varepsilon = 1,\\
&(C^h)^2 \gamma k\mu \int_0^a \int_0^b \left[k_x^2 \sin^2 k_x x \cos^2 k_y y + k_y^2 \cos^2 k_x x \sin^2 k_y y\right] dxdy\\
&= \frac{1}{4}(C^h)^2 abg^2 \gamma k\mu = 1.
\end{aligned}$$

Form which the constants C^s are determined as follows

$$\begin{aligned}
C^e &= \frac{2}{\sqrt{ab}} \frac{1}{g\sqrt{\gamma k\varepsilon}} = \frac{2}{\sqrt{ab}} \frac{1}{g\gamma\sqrt{Y^e}},\\
C^h &= \frac{2}{\sqrt{ab}} \frac{1}{g\sqrt{\gamma k\mu}} = \frac{2}{\sqrt{ab}} \frac{\sqrt{Y^h}}{g\gamma},
\end{aligned} \tag{A5}$$

where $g^2 = k_x^2 + k_y^2$, $k_x = \pi m/a$, $k_y = \pi n/b$, $\gamma = \sqrt{k^2\varepsilon\mu - g^2}$, and $Y^e = k\varepsilon/\gamma$, $Y^h = \gamma/k\mu$ are the wave admittances.

APPENDIX B.

The matrices $\mathbf{T}_1$ and $\mathbf{T}_2$ are the particular transfer matrices of rank 4 of the first and second layers of period. They are

$$\begin{aligned}\mathbf{T}_1 &= \mathbf{T}_{01}\mathbf{P}_1\mathbf{T}_{10} = \begin{pmatrix}\mathbf{T}_1^{hh} & \mathbf{T}_1^{he}\\ \mathbf{T}_1^{eh} & \mathbf{T}_1^{ee}\end{pmatrix},\\ \mathbf{T}_2 &= \mathbf{T}_{02}\mathbf{P}_2\mathbf{T}_{20} = \begin{pmatrix}\mathbf{T}_2^{hh} & 0\\ 0 & \mathbf{T}_2^{ee}\end{pmatrix},\end{aligned} \tag{B1}$$

where $\mathbf{T}_{0j}$ and $\mathbf{T}_{j0}$ $(j = 1, 2)$ are the transfer matrices of the layer interfaces with outer half-spaces, and $\mathbf{P}_j$ are the propagation matrices through the corresponding layer. The elements of the block matrices $\mathbf{T}_{0j}$ and $\mathbf{T}_{j0}$ are determined by solving the boundary-value problem related to the field components (A3). In the block representation (2×2), the transfer matrices of the first layer are

$$\mathbf{T}_{01} = \begin{pmatrix}\mathbf{T}_{01}^{hh} & \mathbf{T}_{01}^{he}\\ \mathbf{T}_{01}^{eh} & \mathbf{T}_{01}^{ee}\end{pmatrix}, \mathbf{T}_{10} = \begin{pmatrix}\mathbf{T}_{10}^{hh} & 0\\ 0 & \mathbf{T}_{10}^{ee}\end{pmatrix}, \mathbf{P}_1 = \begin{pmatrix}\mathbf{E}_1 & 0\\ 0 & \mathbf{E}_1\end{pmatrix}, \tag{B2}$$

$$\begin{aligned}\mathbf{T}_{01}^{hh} =& \Delta^{hh}\begin{pmatrix} k_x^2(Y_0^h + Y_1^h + Y_x^h) + k_y^2C(Y_0^h + Y_1^h + Y_y^h) & k_x^2(Y_0^h + Y_1^h - Y_x^h) + k_y^2C(Y_0^h + Y_1^h - Y_y^h)\\ k_x^2(Y_0^h - Y_1^h + Y_x^h) + k_y^2C(Y_0^h - Y_1^h + Y_y^h) & k_x^2(Y_0^h + Y_1^h - Y_x^h) + k_y^2C(Y_0^h + Y_1^h - Y_y^h)\end{pmatrix},\\ \mathbf{T}_{01}^{he} =& \Delta^{he}\begin{pmatrix}1 & -1\\ -1 & 1\end{pmatrix},\\ \mathbf{T}_{10}^{hh} =& \Delta^{h}\begin{pmatrix}Y_1^h + Y_0^h & Y_1^h - Y_0^h\\ Y_1^h - Y_0^h & Y_1^h + Y_0^h\end{pmatrix},\\ \mathbf{E}_1 =& \begin{pmatrix}\exp(-i\gamma_1 D_1) & 0\\ 0 & \exp(i\gamma_1 D_1)\end{pmatrix},\end{aligned} \tag{B3}$$

where $Y_x^h = iU^+$, $Y_y^h = iU^-C$, $\Delta^{hh} = \Delta^h/(k_x^2 + k_y^2C)$, $\Delta^{he} = k_xk_y(iU^+ - iU^-C)/2\sqrt{Y_0^hY_1^e}(k_x^2 + k_y^2C)$, $\Delta^h = 1/2\sqrt{Y_0^hY_1^h}$ and $C = 1+Mg^2/k^2$. The coefficients of the transfer matrices $\mathbf{T}_{01}^{ee}$, $\mathbf{T}_{01}^{eh}$ and $\mathbf{T}_{10}^{ee}$ are determined from (B3) via interchanging indexes e and h $(e \leftrightarrow h)$, $Y_x^e = iU^-$, $Y_y^e = iU^+/C$ and changing the sign of the matrix elements: $t_{12}^{ee} = -t_{12}^{hh}$, $t_{21}^{ee} = -t_{21}^{hh}$, $t_{12}^{eh} = -t_{12}^{he}$, $t_{21}^{eh} = -t_{21}^{he}$. The elements of the transfer matrices $\mathbf{T}_{02}$, $\mathbf{T}_{20}$ and $\mathbf{T}_2$ of the second layer are determined in the same way from (B2), (B3) via substituting 2 for 1 and assigning $Y_x^h = Y_y^h = Y_x^e = Y_y^e = 0$.

REFERENCES

1. Born, M. and E. Wolf, *Principles of Optics*, Pergamon Press, Oxford, 1968.
2. Yariv, A. and P. Yeh, *Optical Waves in Crystals: Propagation and Control of Laser Radiation*, Wiley, New York, 1984.
3. Sakoda, K., *Optical Properties of Photonic Crystals*, Springer, Berlin, 2001.
4. Gómez, Á., A. Vegas, M. A. Solano, and A. Lakhtakia, "On one- and two-dimensional electromagnetic band gap structures in rectangular waveguides at microwave frequencies," *Electromagnetics*, Vol. 25, No. 5, 437–460, 2005.
5. Khalaj-Amirhosseini, M., "Microwave filters using waveguides filled by multi-layer dielectric," *Progress In Electromagnetics Research*, Vol. 66, 105–110, 2006.
6. Elachi, C., "Waves in active and passive periodic structures: A review," *Proceedings of the IEEE*, Vol. 64, No. 12, 1666–1698, 1976.
7. Yang, F.-R., K.-P. Ma, Y. Qian, and T. Itoh, "A novel TEM waveguide using uniplanar compact photonic-bandgap (UC-PBG) structure," *IEEE Trans. Microwave Theory Tech.*, Vol. 47, No. 11, 2092–2098, 1999.
8. Merrill, M., C. A. Kyriazidou, H. F. Contopanagos, and N. G. Alexópoulos, "Electromagnetic scattering from a PBG material excited by an electric line source," *IEEE Trans. Microwave Theory Tech.*, Vol. 47, No. 11, 2105–2114, 1999.
9. Kirilenko, A. A. and L. P. Mospan, "Reflection resonances and natural oscillations of two-aperture iris in rectangular waveguide," *IEEE Trans. Microwave Theory Tech.*, Vol. 48, No. 8, 1419–1421, 2000.
10. Kyriazidou, C. A., H. F. Contopanagos, and N. G. Alexópoulos, "Monolitic waveguide filters using printed photonic-bandgap materials," *IEEE Trans. Microwave Theory Tech.*, Vol. 49, No. 2, 297–307, 2001.
11. Lytvynenko, L. M. and S. L. Prosvirnin, "Wave reflection by a periodic layered metamaterial — Reflection by a semi-infinite layered structure," *The European Physical Journal-Applied Physics*, Vol. 46, 32608, 2009.
12. Hasar, U. C. and O. Simsek, "An accurate complex permittivity method for thin dielectric materials," *Progress In Electromagnetics Research*, Vol. 91, 123–138, 2009.

13. Siakavara, K. and C. Damianidis, "Microwave filtering in waveguides loaded with artificial single or double negative materials realized with dielectric spherical particles in resonance," *Progress In Electromagnetics Research*, Vol. 95, 103–120, 2009.
14. Hussain, A. and Q. A. Naqvi, "Fractional rectangular impedance waveguide," *Progress In Electromagnetics Research*, Vol. 96, 101–116, 2009.
15. Fallahzadeh, S., H. Bahrami, and M. Tayarani, "A novel dual-band bandstop waveguide filter using split ring resonators," *Progress In Electromagnetics Research Letters*, Vol. 12, 133–139, 2009.
16. Zhang, D. and J.-G. Ma, "The propagation and cutoff frequencies of the rectangular metallic waveguide partially filled with metamaterial multilayer slabs," *Progress In Electromagnetics Research M*, Vol. 9, 35–40, 2009.
17. Levin, L., *Theory of Waveguides*, Newnes-Butterworth, London, 1975.
18. Matthaei, G. L., L. Young, and E. M. T. Jones, *Microwave Filters, Impedance-matching Networks and Coupling Structures*, Artech House, Dedham, Mass., 1980.
19. Pozar, D. M., *Microwave Engineering*, Wiley, Toronto, 1998.
20. Ghorbaninejad, H. and M. Khalaj-Amirhosseini, "Compact bandpass filters utilizing dielectric filled waveguides," *Progress In Electromagnetics Research B*, Vol. 7, 105–115, 2008.
21. Kinowski, D., M. Guglielmi, and A. G. Roederer, "Angular bandpass filters: An alternative viewpoint gives improved design flexibility," *IEEE Trans. Antennas Propag.*, Vol. 43, No. 4, 390–395, 1995.
22. Kazansky, V. B., V. V. Podloznyi, and V. V. Khardikov, "Analysis of scattering by a series of uniform elements by means of the Cayley-Hamilton theorem," *Telecommunications and Radio Engineering*, Vol. 54, Nos. 8–9, 28–39, 2000.
23. Kazanskiy, V. B., V. R. Tuz, and V. V. Khardikov, "Quasiperiodic metal-dielectric structure as a multifunctional control system," *Radioelectronics and Communications Systems*, Vol. 45, No. 7, 38–46, 2002.
24. Birbir, F., J. Shaker, and Y. M. M. Antar, "Chebishev bandpass spatial filter composed of strip gratings," *IEEE Trans. Antennas Propag.*, Vol. 56, No. 12, 3707–3713, 2008.
25. Sivov, A. N., "Electrodynamic theory of a dense plane grating of parallel conductors," *Radiotekh. Elektron.*, Vol. 6, No. 4, 483–495,

1961 (in Russian). [English transl. in *Radio Eng. Electron. Phys.*, Vol. 6, No. 4, 429–440, 1961].

26. Weinstein, L. A., "On the electrodynamic theory of grids," *Elektronika Bol'shikh Moshchnostey*, P. L. Kapitsa and L. A. Weinstein (eds.), Vol. 2, 26–74, Nauka, Moscow, 1963 (in Russian). [English transl. in *High-power Electronics*, 14–48, Pergamon Press, Oxford, 1966].
27. Tretyakov, S., *Analitycal Modeling in Applied Electromagnetics*, Artech House, Boston, London, 2003.
28. Adonina, A. I. and V. V. Shcerbak, "Equivalent boundary conditions at a metal grating situated between two magnetic materials," *Zh. Tekh. Fiz.*, Vol. 34, No. 2, 333–335, 1964 (in Russian). [English transl. in *Sov. Phys. Tech. Phys.*, Vol. 9, 261–263, 1964].
29. Jaggard, D. L. and X. Sun, "Reflection from fractal multilayers," *Opt. Lett.*, Vol. 15, 1428–1430, 1990.
30. Lavrinenko, A. V., S. V. Zhukovsky, K. S. Sandomirskii, and S. V. Gaponenko, "Propagation of classical waves in non-periodic media: Scaling properties of an optical Cantor filter," *Phys. Rev. E*, Vol. 65, 036621, 2002.
31. Chiadini, F., V. Fiumara, I. Gallina, S. T. Johnson, and A. Scaglione, "Cantor dielectric filters in rectangular waveguides," *Electromagnetics*, Vol. 29, No. 8, 575–585, 2009.
32. Tuz, V. R. and V. B. Kazanskiy, "Electromagnetic scattering by a quasiperiodic generalized multilayer Fibonacci structure with grates of magnetodielectric bars," *Waves in Random and Complex Media*, Vol. 19, No. 3, 501–508, 2009.
33. Tuz, V. R., "A peculiarity of localized mode transfiguration of a Cantor-like chiral multilayer," *J. Opt. A: Pure Appl. Opt.*, Vol. 11, 125103, 2009.
34. Ghosh, B., S. N. Sinha, and M. Kartikeyan, "Investigations on fractal frequency selective diaphragms in rectangular waveguide," *International Journal of RF and Microwave Computer-Aided Engineering*, Vol. 20, No. 2, 209–219, 2010.
35. Lamb, H., "On the reflection and transmission of electric waves by a metallic grating," *Proc. London Math. Soc., Ser. 1*, Vol. 29, 523–544, 1898.
36. Dickey, L. J., "High powers of matrices," *ACM SIGAPL APL Quote Quad.*, Vol. 18, No. 2, 96–99, 1987.
37. Tuz, V. R. and V. B. Kazanskiy, "Periodicity defect influence on the electromagnetic properties of a sequence with bi-isotropic

layers," *Progress In Electromagnetics Research B*, Vol. 7, 299–307, 2008.

38. Vytovtov, K. A. and A. A. Bulgakov, "Analytical investigation method for electrodynamics properties of periodic structures with magnetic layers," *Telecommunications and Radio Engineering*, Vol. 65, No. 14, 1307–1321, 2006.
39. Tuz, V. R. and V. B. Kazanskiy, "Depolarization properties of a periodic sequence of chiral and material layers," *J. Opt. Soc. Am. A*, Vol. 25, No. 11, 2704–2709, 2008.
40. Tuz, V. R., M. Yu. Vidil, and S. L. Prosvirnin, "Polarization transformations by a magneto-photonic layered structure in vicinity of ferromagnetic resonance," *J. Opt.*, Vol. 12, 095102, 2010.